npj | regenerative medicine

Brief communication

Published in partnership with the Australian Regenerative Medicine Institute

https://doi.org/10.1038/s41536-025-00417-y

# Genetic compensation response contributes to *Pleurodeles waltl* limb regeneration



Binxu Yin[1,2,3] ✉, Changhao Yu[2,3], Yang Liu[1,3], Hao Cai[2,3], Wencheng Wu[1], Tingting Ye[2], Lei Wang[1], Lujia Xiao[1], Yi Zhu[1], Huaijuan Guo[1], Kun Zhang[1] ✉ & Heng Wang[2] ✉

Hippo-Yap/Taz pathway is essential for tissue regeneration in multiple species. However, we found that in the highly regenerative salamanders, *Yap* knockout does not compromise the limb regeneration due to genetic compensation response (GCR). Specifically, the mutated *Yap* locus derived non-sense mRNA, which was recognized by UPF3A to instruct compensatory *Taz* induction. Blocking *Yap* mRNA or protein indeed inhibits regeneration. GCR could be utilized to maintain the robustness of limb regeneration.

Genetic compensation response (GCR) is a biological phenomenon that contributes to the genetic robustness of an organism, ensuring its fitness and viability when encountering deleterious genetic mutations or variations. GCR helps to explain the paradox observed in animal development where a pronounced phenotype is seen after mRNA or protein knockdown (KD), but no phenotype after DNA knockout (KO), largely due to the compensatory effects of homologous genes[1–4]. Whether this biological paradox also occurs during animal regeneration remains unknown. To address this question, we utilized the salamander limb regeneration model, since salamanders are the only vertebrates that can repeatedly and perfectly regenerate entire limbs throughout life.

The Hippo-Yap/Taz signaling cascade is evolutionarily conserved from Drosophila to humans, and perturbations in this pathway frequently result in defects in tissue development and regeneration[5]. However, in our previously established YAP knockout salamanders, we observed normal limb regeneration upon amputation. This finding contrasts with the limb regeneration defects reported in the *Yap* knockdown assays[6], prompting us to investigate whether the GCR could be responsible for this discrepancy. In the present study, we performed various loss-of-function assays targeting components of the Hippo-Yap/Taz pathway and the GCR process in salamanders to assess the involvement of GCR in limb regeneration.

We utilized previously established *Yap* mutants[7] to compare limb regeneration between KO and wild-type (WT) Iberian ribbed newts (*Pleurodeles waltl*). The mutants were created using CRISPR-Cas9 and maintained in both heterozygous and homozygous forms. A two-base pair deletion in exon 4 caused a frameshift in a reading frame that results in a truncated protein with a premature termination codon (PTC) (Fig. S1). To assess regenerative capacity, we performed amputations at the wrist level in both KO and WT animals (Fig. 1a). Immunostaining showed that YAP protein was highly expressed in the regenerating limbs in WT but was completely absent in KO animals (Fig. S2a), which confirm the high YAP activity during blastema formation[8]. Surprisingly, we found that the regeneration phenotypes of KO limbs appeared normal compared to WT, with no discernible differences in blastema formation or patterning throughout (Fig. 1b). Given that KO animals were smaller in size and the limbs were shorter prior to amputation[7], we measured the length of the regrowing limbs and compared it to the contralateral uninjured limb of the same animal (regenerating/uninjured ratio) to determine the regeneration efficiency. Although the absolute limb length was shorter in the KO animals at 28 dpa (days post amputation) and 42 dpa (Fig. S2b), the relative regenerating efficiency was nearly identical compare to the WT animals (Fig. 1c). The cell proliferation analysis by EdU assay also showed no difference in the proportion of proliferating cells between the KO and WT animals (Fig. 1d). In addition, the expression levels of classical YAP/TAZ target genes, including *CCND*, *CCNE*, *CTGF*, *Cyr61* and *Amotl2*, remained unchanged upon *Yap* knockout (Fig. S2c). Hence, the morphological observations, regeneration efficiency, and cell proliferation rates were all similar between KO and WT animals, suggesting the KO of *Yap* does not impair limb regeneration. This finding is particularly striking given the established role of YAP in tissue regeneration across multiple species[9–11] and even in different tissue within the same species[7]. Therefore, to further investigate the role of YAP in salamander limb regeneration, we employed alternative loss-of-function approaches, such as mRNA or protein inhibition.

We first employed the morpholino oligonucleotides (MO) to inhibit YAP protein translation by binding to the start codon of *Yap* mRNA in WT animals (Fig. S3a). Similar to the KO animals, the YAP protein was dramatically reduced upon MO treatment (Fig. S3b). However, in contrast to

[1]Central Laboratory and Orthopedic Department, Sichuan Academy of Medical Sciences, Sichuan Provincial People's Hospital, University of Electronic Science and Technology of China, Chengdu, China. [2]College of Animal Science, Shandong Provincial Key Laboratory for Animal Germplasm Innovation & Utilization, Shandong Agricultural University, Taian, China. [3]These authors contributed equally: Binxu Yin, Changhao Yu, Yang Liu, Hao Cai.
✉e-mail: yin_binxu@uestc.edu.cn; zhangkun2023@uestc.edu.cn; wangheng@sdau.edu.cn

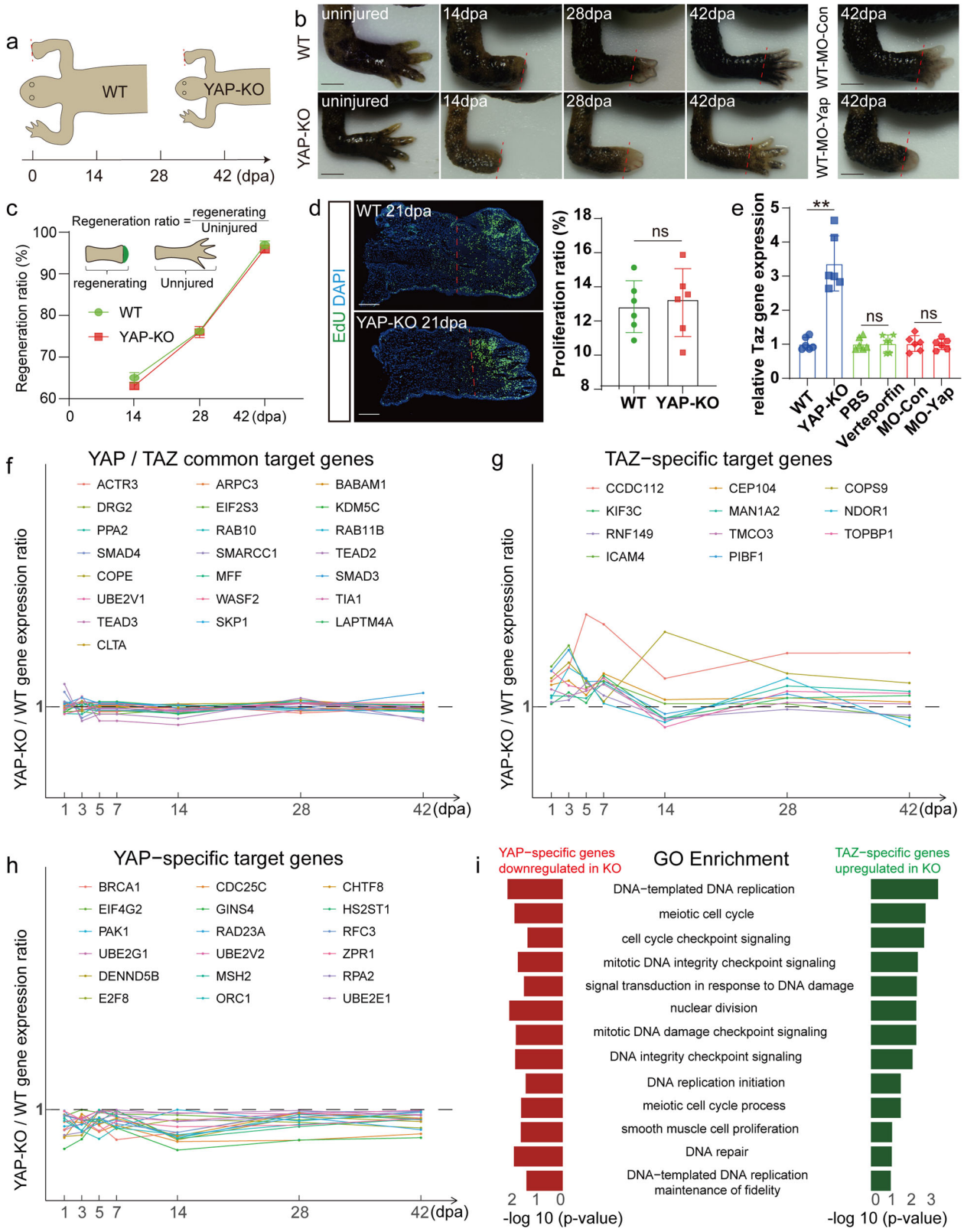


the normal limb regeneration in the KO animals, the MO-Yap-treated animals exhibited severely disrupted limb regeneration (Figs. 1b, S3c), characterized by delayed blastema formation (14–28 dpa) and failed patterning (42–60 dpa). Detailed analysis in MO-Yap limb sections revealed a significant reduction in cell proliferation (Fig. S3d) and compromised cartilage re-formation (Fig. S3e). In addition, the expression of YAP/TAZ target genes, including *CCND*, *CCNE*, *CTGF*, *Cyr61*, and *Amotl2*, was all significantly downregulated (Fig. S3f). To further investigate the role of YAP protein in limb regeneration, we treated WT animals with verteporfin, a small molecule known to promote cytoplasmic retention and degradation of YAP[12]. Verteporfin administration effectively blocked YAP nuclei accumulation and promoted YAP protein degradation (Fig. S4a). The

**Fig. 1 | Genetic compensatory response contributed to limb regeneration.** **a** Experimental scheme of limb regeneration in WT and YAP-KO juvenile newts. **b** Representative pictures demonstrate that the limb regeneration process and morphology are normal in YAP-KO animals (left). Please note the limb regeneration defects at 42 dpa in the Yap-MO treated WT animals (right). **c** The Yap-KO and WT animals showed the same limb regeneration ratio. The length of the regrowing limbs was compared to the contralateral uninjured limb of the same animal (regenerating/uninjured) to determine the relative regeneration efficiency. **d** EdU staining of WT and YAP-KO regenerating limbs at 21 dpa (left) and quantification of cell proliferation (right). **e** The *Taz* expression was induced in YAP-KO, but not in the YAP knockdown animals, including chemical inhibitor verteporfin and Yap-morpholino groups. **f** The transcriptome analysis demonstrated that YAP/TAZ common target genes were largely unchanged. **g** The transcriptome analysis demonstrated that TAZ-specific target genes were upregulated in YAP-KO limbs. **h** The transcriptome analysis demonstrated that YAP-specific target genes were downregulated in YAP-KO limbs. **i** GO analysis of TAZ-specific upregulated genes and YAP-specific downregulated genes showed that many biological functions were overlapped. Scale bar in (**b**): 1 mm. Scale bar in (**d**): 500 μm. Data are mean ± SEM. $n = 6$ animals in (**b**–**e**). $^{*}p < 0.05$, $^{**}p < 0.01$, ns not significant, by *t*-test.

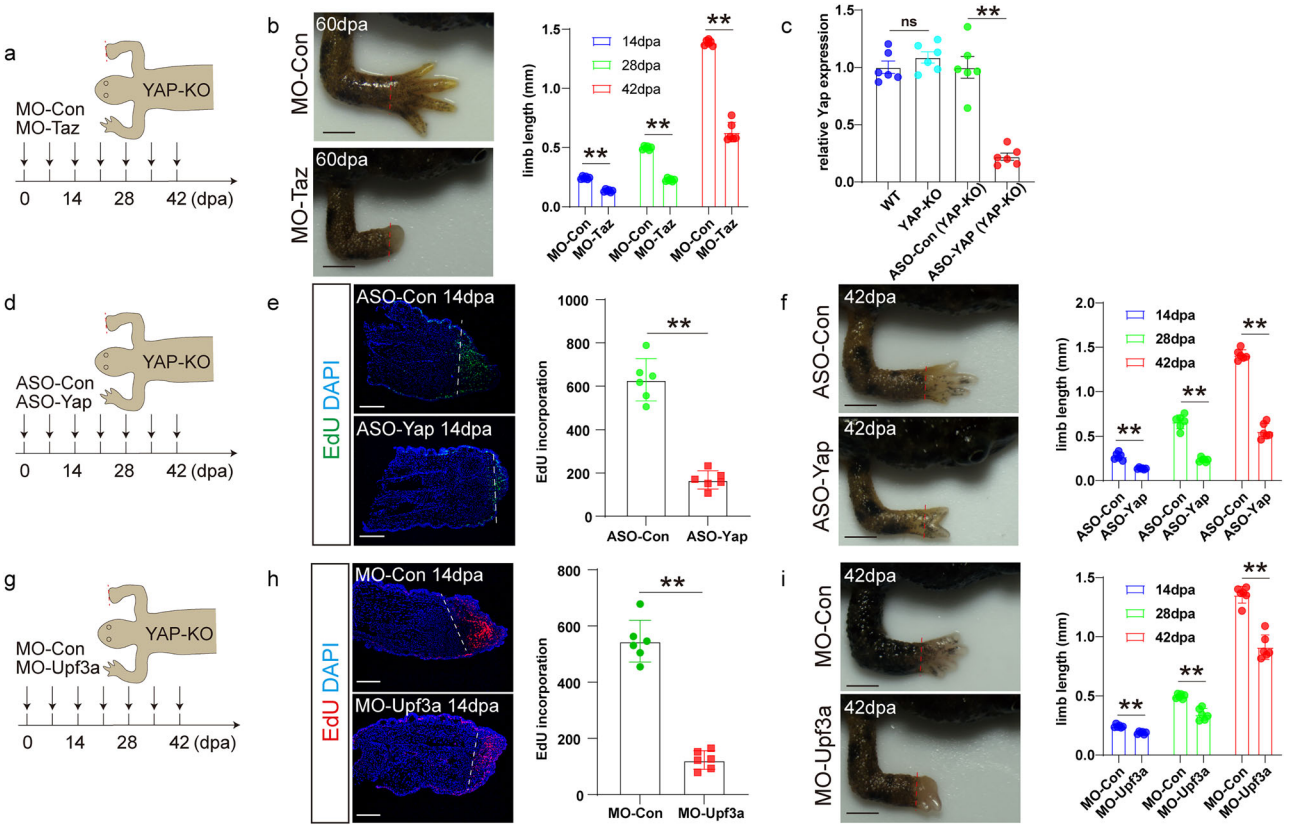


**Fig. 2 | Activation of *Taz* by nonsense *Yap* mRNA via Upf3a contributes to normal limb regeneration in YAP-KO animals.** **a** Experimental scheme of *Taz* inhibition during limb regeneration in YAP-KO animals. **b** Representative pictures (left) showing that blocking *Taz* in YAP-KO animals disrupts limb regeneration as evidenced by failed patterning at 60 dpa. The limb length was significantly shorter than control at different time points (right). Please see Fig. S5c for the detailed limb morphology over the entire regeneration period. $n = 6$. **c** The expression levels of *Yap* mRNA in WT, *Yap* nonsense mRNA in YAP-KO, YAP-KO + ASO-Con, and YAP-KO + ASO-Yap animals. **d** Experimental scheme of nonsense *Yap* mRNA depletion by ASO in YAP-KO animals. **e** EdU staining of ASO-Con and ASO-Yap regenerating limbs at 14 dpa in YAP-KO animals (left) and quantification of cell proliferation (right). **f** Representative pictures (left) show that nonsense *Yap* mRNA elimination in YAP-KO animals disrupts limb regeneration and results in patterning defects. The limb outgrowth length was significantly shorter than control (right). The limb length in Fig. 2f, and Fig. S8c was measured at multiple time points over the entire regeneration period. $n = 6$. **g** Experimental scheme of Upf3a inhibition in YAP-KO animals. **h** EdU staining of MO-Con and MO-Upf3a regenerating limbs at 14 dpa in YAP-KO animals (left) and quantification of cell proliferation (right). **i** Representative pictures (left) show that *Upf3a* inhibition in YAP-KO animals leads to limb regeneration description and patterning defects. The limb outgrowth length in the MO-Upf3a group was significantly shorter than control at different time points during regeneration (right). Please see Fig. S9c for the detailed limb analysis at multiple time points over the entire regeneration period. $n = 6$. Scale bar in (**b**), (**f**), and (**i**): 1 mm. Scale bar in (**e**) and (**h**): 500 μm. Data are mean ± SEM. $n = 6$ animals in (**b**), (**c**), (**e**), (**f**), (**h**), and (**i**). $^{*}p < 0.05$, $^{**}p < 0.01$, ns not significant, by *t*-test.

verteporfin-treated WT animals exhibited severe defects in limb regeneration, including delayed blastema formation and a complete absence of patterning even at 60 dpa (Fig. S4b). The cell proliferation (Fig. S4c), cartilage formation (Fig. S4d), and target gene expression (Fig. S4e) were all markedly inhibited. Therefore, these results confirmed the essential function of YAP protein during limb regeneration[6,13], as demonstrated by both *Yap* mRNA KD and YAP protein inhibition.

The disruption of limb regeneration in YAP-KD but not YAP-KO animals prompted us to hypothesize that the GCR could be responsible for this discrepancy. Indeed, we found the expression of the other Hippo pathway effector *Taz* was significantly induced in the regenerating limbs of YAP-KO animals, but not in any of the WT or knockdown groups (WT, WT + KD, WT + verteporfin) (Fig. 1e). Gene expression analysis revealed that during limb regeneration, TAZ-specific target genes were upregulated in YAP-KO compared to WT animals (Fig. 1g) while YAP-specific genes were downregulated (Fig. 1h). In contrast, the YAP/TAZ common target genes remain largely unchanged (Fig. 1f). Notably, the TAZ-specific target genes were rapidly induced during the early stage of regeneration (1–7 dpa)

(Fig. 1g). Interestingly, the top enriched signaling pathways in both "YAP-specific genes downregulated in KO" and "TAZ-specific genes upregulated in KO" were predominantly associated with cell proliferation and tissue repair process (Fig. 1i). It indicates that the TAZ-specific gene activation compensates for the loss of YAP-specific gene function and could mitigate the deleterious effects caused by the loss of YAP during limb regeneration. These results suggest that the unimpaired limb regeneration in YAP-KO animals is associated with compensatory upregulation of TAZ.

Next, to directly test the occurrence of GCR and the compensatory role of TAZ during limb regeneration, we blocked TAZ function through MO to investigate whether TAZ is necessary for successful limb regeneration in YAP-KO animals. We amputated the YAP-KO limbs and then injected MO-Con and MO-Taz into the regenerating limbs, respectively (Fig. 2a). RT-PCR confirmed that MO-Taz efficiently inhibited the splicing of *Taz* mRNA and thereby blocked the protein translation (Fig. S5a). We validated the efficiency of TAZ inhibition by examining its downstream target genes and found that the expression of YAP/TAZ target genes was all significantly downregulated (Fig. S5b), indicating that TAZ activity was effectively suppressed. As a result, we found the limb regeneration was severely impaired upon MO-Taz treatment as evidenced by the significantly shorter limb outgrowth and failed patterning in the MO-Taz group compared to controls (Figs. 2b, S5c). The cell proliferation (Fig. S5d) and new cartilage formation (Fig. S5e) were both inhibited. These results suggest that the induction of TAZ is essential to compensate for the loss of YAP to ensure successful limb regeneration in YAP-KO animals.

The phenomenon of knockdown/knockout inconsistency has been reported to occur in about 80% of genes during zebrafish development, and the compensatory upregulation of homologous gene(s) could rescue the loss of the mutated gene to maintain normal development[14]. Different molecular mechanisms are involved in the specific induction of the homologous gene, including the Upf1-mediated nonsense mRNA decay (NMD)[2] and Upf3a-mediated premature termination codon (PTC) recognition[3,4]. We found that the amount of *Yap* mRNA was comparable between the KO and WT animals (Fig. 2c), suggesting that the nonsense mRNA generated in KO animals was not efficiently degraded. Furthermore, expression analysis revealed no upregulation of any Upf family genes in the regenerative blastemas of WT animals (Fig. S6), indicating that the Upf pathway is not broadly activated by limb regeneration itself. However, we found significant upregulation of *Upf3a*, but not *Upf1*, *Upf2,* or *Upf3b*, in the regenerating limbs of YAP-KO animals (Fig. S7). It indicates that Upf3a-mediated recognition of PTC-containing transcripts, but not the *Upf1*/*Upf2*/*Upf3b*-mediated degradation of nonsense mRNA, could be the major trigger for GCR activation during limb regeneration. We tested this hypothesis by either eliminating the PTC-containing nonsense mRNA or inhibiting UPF3A function.

First, we tested whether the presence of PTC-containing nonsense mRNA was necessary for the successful limb regeneration in YAP-KO animals by using antisense oligonucleotides (ASO) to eliminate the mutated *Yap* mRNA. The YAP-KO regenerating limbs were injected with ASO-Yap and ASO-Con, respectively (Fig. 2d), and RT-qPCR confirmed the depletion of the mutant mRNA molecules by ASO-Yap (Fig. 2c). We also checked the expression of PTC-recognizing Upf3a following the reduction of nonsense mRNA. Interestingly, unlike the upregulation of *Upf3a* observed in the presence of abundant nonsense mRNA, *Upf3a* remained unchanged after ASO-mediated depletion of Yap nonsense mRNA (Fig. S8a). Hence, it seems that the expression of *Upf3a* is correlated with the quantity of PTC-containing nonsense mRNA, and a threshold level of nonsense mRNA transcripts may be required for the proper induction and operation of *Upf3a*. Further analysis revealed that upon depletion of Yap nonsense mRNA, the expression of *Taz* and representative YAP/TAZ target genes was significantly suppressed (Fig. S8b). Correspondingly, ASO-Yap treatment severely impaired cell proliferation (Fig. 2e), blastema formation, and limb patterning in YAP-KO animals (Fig. 2f, Fig. S8c). These results suggest that the presence of *Yap* nonsense mRNA in YAP-KO animals is crucial for triggering GCR to increase the transcription of *Taz* to support limb regeneration.

Among the RNA surveillance Upf family members, only *Upf3a* was significantly upregulated in the YAP-KO animals (Fig. S7). Upf3a has been reported to specifically activate expression of homologous genes in organ development through epigenetic mechanisms[3,4]. We used MO to block *Upf3a* to determine whether UPF3A was responsible for the compensatory expression of *Taz* during limb regeneration in YAP-KO animals (Fig. 2g). We found that MO-Upf3a efficiently inhibited the exon-intron splicing of *Upf3a* (Fig. S9a) and thereby prevented the proper translation of Upf3a. RT-qPCR showed that the expression levels of *Taz* and YAP/TAZ downstream target genes were all significantly downregulated, indicating that inhibition of *Upf3a* blocked the activation of GCR and *Taz* expression (Fig. S9b). Consequently, the MO-Upf3a treated animals showed disrupted cell proliferation (Fig. 2h), delayed blastema formation, and patterning defects during limb regeneration (Figs. 2i, S9c). Taken together, these results suggest that both the presence of nonsense *Yap* mRNA and the functional UPF3A are necessary for the activation of *Taz* to ensure normal limb regeneration in YAP-KO animals. Our data suggest that UPF3A-mediated PTC recognition is the major mechanism of GCR during limb regeneration (Fig. S10). In light of these results, we further hypothesize that GCR-mediated regulatory interference may extend to additional genes involved in tissue regeneration. To rigorously evaluate gene function and regenerative outcomes, the application of multiple independent loss-of-function strategies is recommended.

Previous studies suggest that animals utilize GCR to cope with harmful germline genetic mutations in order to ensure the successful development and survival of the individual. The current study in salamanders demonstrates another aspect of genetic robustness of the organism under adverse conditions, such as injury: the GCR is utilized to ensure the successful limb regeneration to regain functional limbs, which was vitally important for the mobility and viability of the animal (Fig. S11). Further studies are needed to determine whether this potent "regeneration GCR" was exclusive to the highly regenerative salamanders or could be intentionally stimulated in other species to boost tissue repair and regeneration.

## Methods

### Ethics statement

All procedures were carried out in accordance with the Institutional Animal Care and Use Committee of Shandong Agricultural University (ethics approval No.: 2018-0125).

### Animal husbandry, limb amputation, and chemical administration

Iberian ribbed newts, *Pleurodeles waltl,* were maintained in filtered tap water at 22–24 °C under natural light cycles. The juvenile WT and YAP-KO (F2) animals were about 4 months old (Approximately 1 month after metamorphosis). Prior to surgery, juvenile newts were anesthetized with 0.2% tricaine (Sigma, A5040)[15]. All amputations are carried out at the wrist of the limb. For EdU-labeling, animals were injected intraperitoneally with 50 mg/kg 12 h before tissue collection[16]. Verteporfin (TOPSCIENCE, T3112) was administered intraperitoneally at 20 mg/kg in newts to inhibit YAP nuclear translocation.

### Morpholino and antisense oligonucleotide injection

The morpholinos (MO) were provided by Gene Tools (Oregon, USA). All MOs were conjugated with green fluorescent modifications. For newt limbs, 100 nL (125 μM) MOs were injected (once every 7 days) into the regenerating limb through glass microcapillaries and PV830 PicoPump, followed by electroporation. Antisense oligonucleotides (ASO) were used to degrade the nonsense *Yap* mRNA, and all ASO were provided by RiboBio (Guangzhou, China). All ASOs were labeled with red fluorescent modifications. For newt limbs, 100 nL (125 μM) ASOs were injected (once every 7 days) into the limb with glass microcapillaries and PV830 PicoPump. The MOs and ASOs used in this study are listed in Supplementary Table 1.

### Quantitative qPCR and RT-PCR

Approximately 2 mm length of limb tissue was collected from uninjured/injured WT and YAP-KO limbs at 0 dpa and 4 dpa, respectively. The

removed tissue was placed in a petri dish, poured with PBS to remove the blood cells. Total RNA was extracted by using Trizol reagent (Simgen). The cDNA was synthesized by using NovoScript®Plus All-in-one 1st Strand cDNA Synthesis SuperMix (gDNA Purge) (Novoprotein). qRCR assay was performed by using a Hieff qPCR SYBR Green MIX (Yeasen, 11201ES08) on a BIO-RAD CFX384 real-time PCR system. The mixture was incubated at 50 °C for 15 min, 75 °C for 5 min. The qPCR conditions were: initial denaturation at 95 °C for 5 min, followed by 39 cycles of 95 °C for 20 s, 60 °C for 20 s, and 72 °C for 20 s. RT-PCR was used to test the efficiency of MO. The relative amount of *Yap* (nonsense mRNA), *Taz*, *CCND*, *CCNE*, *CTGF*, *Cyr61,* and *Amotl2* mRNA was normalized to the amount of actin, respectively. The $2^{-\Delta\Delta Ct}$ method was used for the evaluation of relative quantification of target gene expression. All primers used in this study are listed in Supplementary Table 2.

### Tissue sectioning, immunofluorescence, and EdU staining

Frozen sections (6–8 μm) were thawed at room temperature and fixed in 4% formaldehyde for 5 min. The sections were then blocked with 10% goat serum in 0.1% Triton-X for 30 min at room temperature. The tissue sections were incubated with primary antibodies overnight at 4 °C and the corresponding secondary antibodies conjugated to Alexa Fluor 488 or 555 (Invitrogen) for 1 h. The sections were washed in PBS three times between different treatments. Primary antibodies used are as follows: anti-YAP (Cell Signaling Technology-D8H1X, 1:100), anti-Collagen 2 (DSHB, 1:20), anti-MF20-488 (eBioscience, 1:500). EdU staining was performed by incubating the sections with 100 mmol/L Tris, 1 mmol/L CuSO4, 10 mmol/L fluorescent azide, and 100 mmol/L ascorbic acid for 30 min[17]. Once all washing steps were completed, the coverslips were counter-stained with 50 ng/mL 4′, 6-diamidino-2-phenylindole (DAPI). A confocal fluorescence microscope (Zeiss LSM710) was used to examine and image the sections.

### RNA-seq analysis

For quality control of RNA-seq data, we used Trimmomatic (version 0.39) to remove low-quality sequences and STAR (version 2.7.11b) to perform read alignment by mapping reads to the reference genome aPleWal1.hap1 (https://ftp.ncbi.nlm.nih.gov/genomes/all/GCF/031/143/425/GCF031143425.1_aPleWal1.hap1.20221129/). The number of aligned reads was quantified using HTSeq (version 2.0.5) together with the gene annotation document GCF031143425.1aPleWal1.hap1.20221129genomic.gtf. The read counts were converted to TPM values. We calculated the relative expression of genes in the YAP-KO group using the TPM values of genes in the WT group as a benchmark. Finally, the multi-gene line plot was completed using the R programming language (version 4.4.1) and the ggplot2 package. The gene and protein nomenclature were standardized[18]. For basic analyses, including PCA and Correlation analysis, see Fig. S12a–o. YAP-specific target genes, TAZ-specific target genes, and YAP/TAZ co-target genes were selected according to http://chip-atlas.org[19]. We retrieve the YAP and TAZ peaks located within ±1 kb of the transcription start site (TSS) to identify high-confidence YAP and TAZ target genes. The two gene sets were overlapped to identify YAP-specific, TAZ-specific, and YAP/TAZ co-target genes. We compare the gene expression in YAP-KO to WT to select the most differentially expressed genes for GO analysis.

### Data analysis

The animal experiments were not randomized. No statistical method was used to predetermine sample size. No samples were excluded from the statistical analysis. All limb samples were from at least 3 different individuals with either left or right limb amputated. For image analysis, each limb sample was assayed with at least three different sections, with one view on each section. The exact biological repeats (animals) were indicated in each figure legend. Data are presented as the mean ± standard error of the mean (SEM). Statistical differences were analyzed by Student's *t*-test. Statistical analyses were performed using GraphPad Prism v8.0.

## Data availability

The RNA-seq datasets generated and analyzed during the current study are available from the NCBI database PRJNA1223625.

Received: 14 February 2025; Accepted: 19 May 2025;
Published online: 31 May 2025

## References

1. Rossi, A. et al. Genetic compensation induced by deleterious mutations but not gene knockdowns. *Nature* **524**, 230–233 (2015).
2. El-Brolosy, M. A. et al. Genetic compensation triggered by mutant mRNA degradation. *Nature* **568**, 193–197 (2019).
3. Ma, Z. et al. PTC-bearing mRNA elicits a genetic compensation response via Upf3a and COMPASS components. *Nature* **568**, 259–263 (2019).
4. Peng, J. Gene redundancy and gene compensation: an updated view. *J. Genet. Genomics* **46**, 329–333 (2019).
5. Moya, I. M. & Halder, G. Hippo–YAP/TAZ signalling in organ regeneration and regenerative medicine. *Nat. Rev. Mol. Cell Biol.* **20**, 211–226 (2019).
6. Bay, S., Öztürk, G., Emekli, N. & Demircan, T. Downregulation of Yap1 during limb regeneration results in defective bone formation in axolotl. *Dev. Biol.* **500**, 31–39 (2023).
7. Yin, B. et al. Developmental switch from morphological replication to compensatory growth for salamander lung regeneration. *Cell Prolif.* **56**, 1–14 (2023).
8. Edwards-Jorquera, S. et al. Mechanical control of tissue growth during limb regeneration. *bioRxiv*. https://doi.org/10.1101/2025.04.07.647008 (2025).
9. Xin, M. et al. Hippo pathway effector Yap promotes cardiac regeneration. *Proc. Natl Acad. Sci. USA***110**, 13839–13844 (2013).
10. Xie, C. et al. Astrocytic YAP promotes the formation of glia scars and neural regeneration after spinal cord injury. *J. Neurosci.* **40**, 2644–2662 (2020).
11. Fan, S. et al. YAP-TEAD mediates PPAR α–induced hepatomegaly and liver regeneration in mice. *Hepatology* **75**, 74–88 (2022).
12. Zhang, X. et al. Targeting downstream subcellular YAP activity as a function of matrix stiffness with Verteporfin-encapsulated chitosan microsphere attenuates osteoarthritis. *Biomaterials* **232**, 119724 (2020).
13. Hayashi, S., Tamura, K. & Yokoyama, H. Yap1, transcription regulator in the Hippo signaling pathway, is required for Xenopus limb bud regeneration. *Dev. Biol.* **388**, 57–67 (2014).
14. Kok, F. O. et al. Reverse genetic screening reveals poor correlation between morpholino-induced and mutant phenotypes in zebrafish. *Dev. Cell* **32**, 97–108 (2015).
15. Cai, H., Peng, Z., Ren, R. & Wang, H. Efficient gene disruption via base editing induced stop in newt Pleurodeles waltl. *Genes* **10**, 837 (2019).
16. Peng, Z. et al. Altered metabolic state impedes limb regeneration in salamanders. *Zool. Res.* **42**, 772–782 (2021).
17. Ma, T. et al. Transdifferentiation of fibroblasts into muscle cells to constitute cultured meat with tunable intramuscular fat deposition. *eLife* **13**, RP93220 (2024).
18. Yun, M. H., Hayashi, T. & Simon, A. Standardized gene and genetic nomenclature for the newt Pleurodeles waltl. *Dev. Dyn.* **251**, 911–912 (2022).
19. Oki, S. et al. ChIP-Atlas: a data-mining suite powered by full integration of public ChIP-seq data. *EMBO Rep.* **19**, 1–10 (2018).

## Acknowledgements

This study was supported by National Science Foundation of China (31771617), Shandong Provincial Natural Science Foundation (ZR2024MC096), NSFC (32101517, 82022033), Sichuan Provincial Science and Technology Program (2024NSFJQ0048, 2025ZNSFSC0987), Research Fund of Sichuan Academy of Medical Sciences and Sichuan Provincial

People's Hospital (24QNPY026), Taishan Scholar Program, Scientific Research Innovation Team of Young Scholar of Shandong.

## Author contributions

B.Y., H.W., and K.Z. conceived and designed the study. B.Y., C.Y., Y.L., and H.C. prepared the data. B.Y., C.Y., Y.L., W.W., H.C., T.Y., L.W., L.X., Y.Z., H.G., K.Z., and H.W. analyzed the data and wrote the paper. All authors read and approved the final version of the manuscript.

## Competing interests

The authors declare no competing interests.

## Additional information

**Supplementary information** The online version contains supplementary material available at https://doi.org/10.1038/s41536-025-00417-y.

**Correspondence** and requests for materials should be addressed to Binxu Yin, Kun Zhang or Heng Wang.